Hydrothermal synthesis, characterization and optical properties of ZnO nanosheets

QUN MA, YONGQIAN WANG*, JUNHAN KONG, HANXIANG JIA, JUN HAN
Faculty of Materials Science and Chemistry, China University of Geosciences, Wuhan, China, 430074

ZnO nanosheet was successfully synthesized on a large scale with a facile and economic hydrothermal method without the assist of template and substrate. The obtained samples were investigated with multiply technique. The sample is composed of a large number of nanosheets with irregular order and is indexed to hexagonal wurtzite ZnO structure. The formation of ZnO nanosheets can be attributed to the absorption of OH^- onto the polar plane of ZnO crystal. Photoluminescence spectrum indicates that the as-prepared ZnO nanosheets only emit ultraviolet (UV) light centered at 398 nm and may have potential application in the high-quality optical devices.

(Received October 24, 2014; accepted September 29, 2016)

Keywords: ZnO nansoheets, Hydrothermal synthesis, Optical properties, Growth mechanism

1. Introduction

Over the past years, Metal-oxides (ZnO, TiO_2, etc) are considered to be some of the most fascinating functional materials due to their outstanding physical and chemical properties and have been widely used in many applications in our daily life [1-4]. Nowadays, zinc oxide (ZnO) has been a versatile and well-studied material due to its direct band-gap of 3.3 eV at room temperature and large exciton binding energy of 60 meV. Since the unique optical and electrical properties, ZnO has attracted numerous attention and efforts for its suitability and versatility in potential applications such as ultraviolet (UV) light emitters, transparent electronic, sensors and photovoltaic devices [5-6]. For example, Yang et al. demonstrated that the piezo-phototronic effect can largely enhance the efficiency of a hybridized inorganic/organic LED made of a ZnO nanowire/p-polymer structure [7]. Tang et al. synthesized a kind of flower-like ZnO nanostructures with good selectivity to toluene and demonstrated it possess potential application as sensors [8]. Catellani et al. found it that ZnO can be used as high performance transparent conductive oxides [9]. Fu et al. investigated the tunable size and sensitization of ZnO nanoarrays as electron transport layers for enhancing photocurrent of photovoltaic devices [10]. Besides, ZnO has been considered to be a more favorable UV emitting phosphor than GaN thanks to its large exciton binding energy (60 meV) which results in a reduced UV lasing threshold, yielding higher UV emitting efficiency at room temperature. Considering excellent physical properties and the motivation of devices miniaturization of ZnO nanomaterials, great contributions and efforts has been focused on the fabrication, characterization and device applications of ZnO nanomaterials with diverse structure and morphology.

An assortment of ZnO nanostructures, such as nanosheets, nanorods, nanowires, nanobelts and nanotubes has been successfully synthesized via various methods [11-14]. For example, Menzel et al. reported ionic liquid assisted growth of ultra-long ZnO nanowires from thermal chemical vapor deposition [15]. Wang et al. studied the controllable synthesis of ZnO nanostructures using hydrothermal electrodeposited method [16]. Zou et al. reported the synthesis of ZnO nanotubes by thermal evaporation and studied their oxygen vacancy-related photocatalytic properties [17]. However, the above- mentioned methods often require sophisticated instrument and cruel conditions. Hydrothermal method as a facile and economical technique has been developed rapidly over the past years [18-19]. In hydrothermal technique, the sizes and shapes of ZnO nanocrystals which are key factors that determine the optical and electrical properties of ZnO can be controlled by the alteration of hydrothermal conditions. Currently, hydrothermal method has been the most promising technique to synthesize diverse size and shapes of ZnO nanocrystals. However, many researchers have concentrated on synthesizing ZnO nanocrystals via hydrothermal method with a template, substrate or seeds, which requires a complicated process and conditions and can non-reproducible. Little work was reported to synthesize ZnO nanocrystals through hydrothermal method without using the template or substrate.

In our work, we have developed a facile and cost-effective way which is free from template or substrate to grow ZnO nanosheets. Compared with other techniques, this method is more commercially viable for industrial

applications. Moreover, we also investigated the structural and optical properties of ZnO nanosheets. A reasonable growth mechanism for ZnO nanosheets was proposed from the view of crystal growth.

2. Experimental section

2.1. Synthesis of ZnO nanosheets

All chemical reagents were of analytical grade and used with no further purification. Our experimental process as follows: zinc acetate dehydrate ($(CH_3COO)_2Zn\cdot 2H_2O$) used as precursor for this synthesis, which was dissolved into 100 mL deionized water to form a transparent solution. And then, sodium hydroxide (NaOH) was added into the solution to provide OH^-. The concentrations of zinc acetate and sodium hydroxide are 0.2 M and 1.0 M, respectively. After stirring for 1 hour, the turbid solution was transferred into autoclaves, which was heated and maintained at 150 ℃ for 12 hours. Subsequently, the final white precipitate was separated by centrifugation, and washed with deionized water and anhydrous ethanol several times to remove the ions possibly remaining in the final product, and finally dried at 60 °C for 6 h in air.

2.2. Characterization

The crystal phase of the product was characterized by X-ray diffraction (XRD, D8 Advanced XRD, Bruker AXS). The general morphologies of the synthesized ZnO samples were investigated by using field emission scanning electron microscopy (FESEM, U8010, HITACHI). The SEM samples were prepared with a thin amorphous gold on their surface. The room temperature photoluminescence (PL) spectra of the sample were measured by using fluorescence spectrophotometer (F-4500, HITACHI) equipped with a Xe lamp (Excitation wavelength is 249 nm).

3. Results and discussion

3.1. Phase and morphology characterization of ZnO nanosheets

The FESEM images of ZnO nanosheets are shown in Fig. 1a and b. A low-magnification view of the products was shown in Fig. 1a and a high-magnification shown in Fig. 1b. It can be seen clearly that the sample consists of a large number of nanosheets. The nanosheets connect with each other and have irregular structure. Meanwhile, we can observe that the product is fine-grained and contain numerous developed grain boundaries and free surfaces. There were some reports that the physical properties of pure nanograined ZnO depend on the existence of defects like free surfaces and grain boundaries [20-21]. That is to say, the existence of surfaces and grain boundaries is critically important for the physical properties of ZnO. Therefore, it can be inferred that the as-prepared ZnO nanosheets may be excellent physical properties [22].

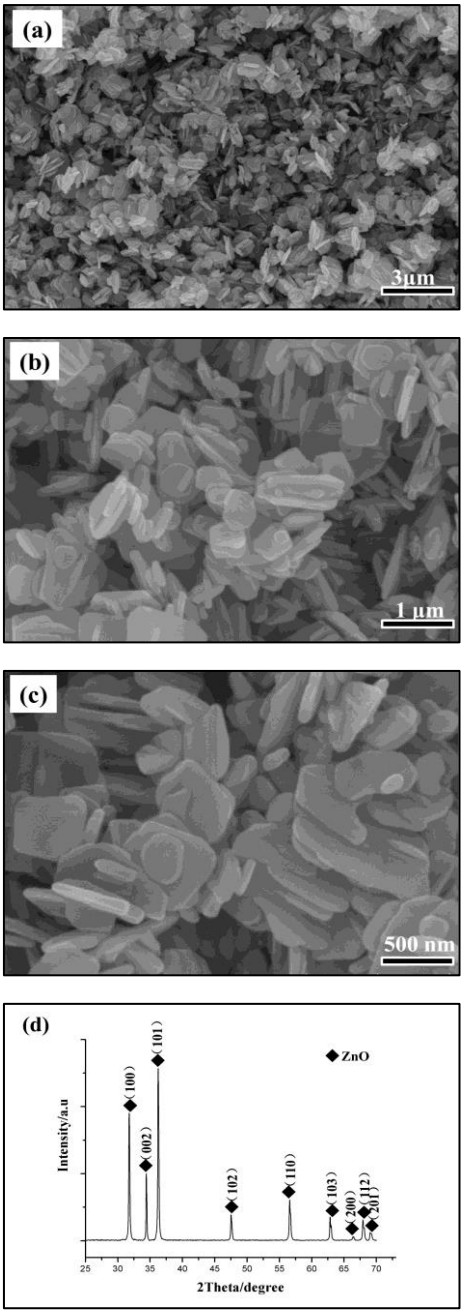

Fig. 1. FESEM images and XRD pattern of ZnO nanosheets synthesized from the facile hydrothermal process, (a) low-magnification FESEM image, (b, c) high-magnification FESEM images, (d) XRD pattern

To investigate the phase structure of ZnO nanosheets, XRD diffraction was employed. Fig. 2 shows the XRD pattern. The diffraction peaks of ZnO nanosheets are indexed the diffraction faces of (100), (002), (101), (102),

(110), (103), (200), (112) and (201), respectively. It can be founded that all of the diffraction peaks match well with the diffraction pattern of typical hexagonal wurtzite ZnO structure (JCPDS Card NO.89-7102). No diffraction peaks from any other impurities were indexed, which confirms that the synthesized product was high pure hexagonal ZnO crystal. Besides, as shown in the XRD pattern, we can also acquire information about that the ZnO nanosheets are well crystallized. Moreover, on the basis of the Scherrer equation, the average crystallite size of obtained ZnO nanosheets was estimated to be 6.2 nm.

3.2. Formation mechanism of the ZnO nanosheets

Herein, a possible mechanism was discussed. It is well know that, the formation process of ZnO in aqueous solution is supported through the following reactions [23-25].

$$Zn^{2+} + 2OH^- = Zn(OH)_2 \downarrow \quad (1)$$

$$Zn(OH)_2 + 2OH^- = Zn(OH)_4^{2-} \quad (2)$$

$$Zn(OH)_4^{2-} \rightarrow ZnO \downarrow + H_2O + 2OH^- \quad (3)$$

In the synthesis systems, white $Zn(OH)_2$ precipitate formed when adding OH^- into aqueous solution with Zn^{2+}, and a homogenous solution including $Zn(OH)_4^{2-}$ ions was obtained when $Zn(OH)_2$ precipitate was dissolved by OH^-. Subsequently, with the dehydration of $Zn(OH)_4^{2-}$ ions, ZnO nuclei were formed and followed by a crystal growth process. At this juncture, choosing suitable hydrothermal conditions can control the size and structure of ZnO nanocrystals.

Fig. 2 illustrates the molecule structure of typical hexagonal wurtzite ZnO crystal. It has been reported that the (0001) and (000-1) faces of ZnO crystal have equal reticular density but vary in the composition of the outermost atomic layer [26]. From Fig. 2, it can be seen that the outermost layer of the positive face (0001) consists of Zn^{2+} ions and the outmost layer of the negative face (000-1) contains O^{2-}. The crystal faces (0001) and (000-1) have a charge of the same magnitude [27-28].

Through above analysis, a possible growth mechanism was obtained. When OH^- ions were added into the aqueous solution containing Zn^{2+} ions, the ZnO nuclei were formed and followed by the crystal growth, as shown equal (1), (2) and (3). It is well known that the growth of crystals was effected by its instinct and ambient conditions. In the hydrothermal system, temperature, reaction time and the concentration of OH^- ions are the key factor to the size and morphology of ZnO crystal. In general, the growth of ZnO crystal tends to be along c-axis ([0001] or [000-1] direction) and form ZnO nanorods using the hydrothermal method. The reason why nanosheets formed was that the growth of c-axis was limited thanks to the adsorption of OH^- onto the (0001) or (000-1) plane. According to the reaction, 0.2 M of Zn^{2+} only needed 0.4 M of OH^-. The rest of 0.6 M of OH^- distributed in the solution and was absorbed onto the (0001) plane, which results in the limitation of growth of ZnO crystal along c-axis[29]. Therefore, the primary ZnO nanosheets formed in the solution. The existence of boundaries and defects in the primary nanosheets would provide new sites for secondary nucleation and growth, which results in the formation of secondary nanosheets, as shown in Fig. 1 (a), (b) and (c) [30-31].

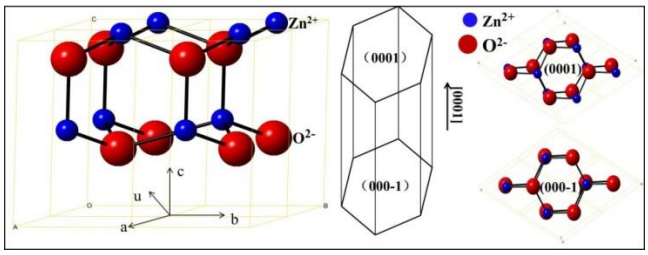

Fig. 2. Molecule structure of ZnO crystal

3.3. Optical properties characterization of ZnO nanosheets

The room temperature photoluminescence (PL) spectrum of the above-mentioned ZnO nanosheets, shown in Fig. 3, was recorded with an excitation wavelength of 249 nm. The PL spectrum exhibits a strong near band edge ultraviolet (UV) emission peak at ~398 nm, which is attributed the radiative recombination of a hole in the valence band and an electron in the conduction band (excitonic emission) [32]. In the spectrum, no other peaks such as blue emission (~468 nm) and green emission (~530 nm) are observed, which indicates ZnO nanosheets fabricated via hydrothermal process may be high crystalline perfection [33-34]. It is reasonably believed that the as prepared ZnO nanosheets possess high-quality optical properties thanks to only emission of UV light.

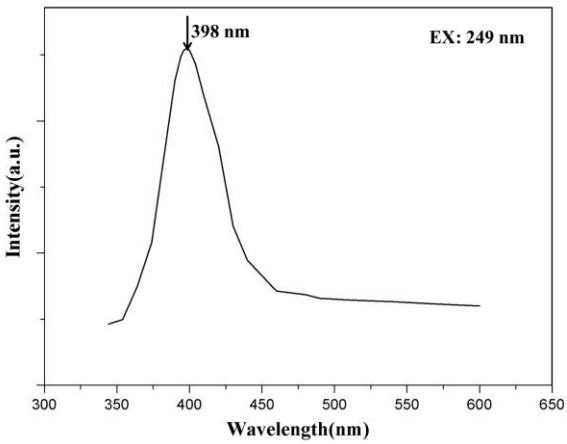

Fig. 3. Room-temperature photoluminescence spectrum of ZnO nanosheets

4. Conclusions

In summary, ZnO nanosheets have been synthesized on a large scale through a facile and economic hydrothermal technique without the assist of template and substrate. The as-prepared ZnO samples are composed of plenty of nanosheets with irregular arrange. The ZnO crystals exhibit typical hexagonal wurtzite ZnO structure. The formation of ZnO nanosheets is attributed to the absorption of OH^- onto the (0001) or (000-1) polar plane of ZnO crystal, which limit the growth of ZnO crystal along the *c* axis direction. The result of photoluminescence indicates that the as-prepared ZnO nanosheets possess high-quality optical properties and only emit ultraviolet (UV) light and may have potential application in optical devices.

References

[1] R. S. Devan, R. A. Patil, J. H. Lin, et al., Advanced Functional Materials **22**(16), 3326 (2012).
[2] J. Zhang, B. Wu, L. Huang, et al., Journal of Alloys and Compounds **661**, 441 (2016).
[3] W. Han, L. Ren, Z. Zhang, et al., Ceramics International **41**(6), 7471 (2015).
[4] W. Han, L, Ren, X. Qi, et al. Applied Surface Science **299**, 12 (2014).
[5] A. L. Zou, L. Z. Hu, Y. Qiu, et al., Journal of Materials Science: Materials in Electronics **26**(7), 4908 (2015).
[6] D. I. Son, B. W. Kwon, J. Do Yang, et al., Nano Research **5**(11), 747 (2012).
[7] Q. Yang, Y. Liu, C. Pan, et al., Nano letters **13**(2), 607 (2013).
[8] W. Tang, J. Wang, Sensors and Actuators B: Chemical **207**, 66 (2015).
[9] A. Catellani, A. Ruini, A. Calzolarim, Journal of Materials Chemistry C **3**(32), 8419 (2015).
[10] H. Fu, L. Tan, Y. Shi, et al., Journal of Materials Chemistry C **3**(4), 828 (2015).
[11] M. N. Cardoza-Contreras, J. M. Romo-Herrera, L. A. Ríos, et al. Sensors **15**(12), 30539 (2015).
[12] R. Krishnapriya, S. Praneetha, A. V. Murugan, New Journal of Chemistry 2016.
[13] C. Han, Z. Chen, N. Zhang, et al., Advanced Functional Materials **25**(2), 221 (2015).
[14] Y. Wang, Q. Ma, H. Jia, et al. Ceramics International **42**(9), 10751 (2016).
[15] A. Menzel, K. Komin, Y. Yang, et al., Nanoscale **7**(1), 92 (2015).
[16] Y. Wang, J. Yang, Y. Li, et al., Materials Chemistry and Physics **153**, 266 (2015).
[17] C. Zou, F. Liang, S. Xue, Research on Chemical Intermediates **41**(8), 5167 (2015).
[18] J. Zhang, P. Liu, Z. Lu, et al., Journal of Alloys and Compounds **632**, 133 (2015).
[19] W. Han, L. Ren, L. Gong, et al., ACS Sustainable Chemistry & Engineering **2**(4), 741 (2014).
[20] A. B. Djurišić, X. Chen, Y. H. Leung, et al., Journal of Materials Chemistry **22**(14), 6526 (2012).
[21] S. Maiti, S. Pal, K. K. Chattopadhyay, Cryst. Eng. Comm. **17**(48), 9264 (2015).
[22] Z. Wang, X. Qian, J. Yin, et al., Langmuir **20**(8), 3441 (2004).
[23] W. J. Li, E. W. Shi, W. Z. Zhong, et al., Journal of crystal growth **203**(1), 186 (1999).
[24] S. W. Bian, I. A. Mudunkotuwa, T. Rupasinghe, et al. Langmuir **27**(10), 6059 (2011).
[25] P. Li, H. Liu, B. Lu, et al., The Journal of Physical Chemistry C **114**(49), 21132 (2010).
[26] J. Liu, Z. Y. Hu, Y. Peng, et al., Applied Catalysis B: Environmental **181**, 138 (2016).
[27] Y. Chen, L. Zhang, L. Ning, et al., Chemical Engineering Journal **264**, 557 (2015).
[28] F. Meng, N. Hou, S. Ge, et al., Journal of Alloys and Compounds **626**, 124 (2015).
[29] Y. Ding, Z. L. Wang, Micron **40**(3), 335 (2009).
[30] J. C. Fan, K. M. Sreekanth, Z. Xie, et al., Progress in Materials Science **58**(6), 874 (2013).
[31] S. J. Chen, Y. C. Liu, C. L. Shao, et al., Advanced Materials **17**(5), 586 (2005).
[32] N. Kiomarsipour, R. S. Razavi, Ceramics International, **40**(7), 11261 (2014).
[33] D. Sahu, N. R. Panda, B. S. Acharya, et al., Optical Materials **36**(8), 1402 (2014).
[34] V. Kumar, V. Kumar, S. Som, et al., Journal of colloid and interface science **428**, 8 (2014).

*Corresponding author: cugwyq@126.com